

**LETTER**

# Single nano-hole as a new effective nonlinear element for third-harmonic generation

**P N Melentiev<sup>1</sup>, T V Konstantinova<sup>1</sup>, A E Afanasiev<sup>1</sup>, A A Kuzin<sup>2</sup>,  
A S Baturin<sup>2</sup>, A V Tausenev<sup>3</sup>, A V Konyaschenko<sup>3</sup> and V I Balykin<sup>1</sup>**

<sup>1</sup> Institute for Spectroscopy, Russian Academy of Sciences, Phizicheskaya street 5, Troitsk, Moscow, 142190, Russia

<sup>2</sup> Moscow Institute of Physics and Technology, Institutskiy per., 9, Dolgoprudniy, Moscow region, 141700, Russia

<sup>3</sup> Avesta Project Ltd, Troitsk, Moscow, 142190, Russia

E-mail: [balykin@isan.troitsk.ru](mailto:balykin@isan.troitsk.ru)

Received 27 September 2012, in final form 22 January 2013

Accepted for publication 20 March 2013

Published 7 June 2013

Online at [stacks.iop.org/LPL/10/075901](http://stacks.iop.org/LPL/10/075901)

## Abstract

In this letter, we report on a particularly strong optical nonlinearity at the nanometer scale in aluminum. A strong optical nonlinearity of the third order was demonstrated on a single nanoslit. Single nanoslits of different aspect ratio were excited by a laser pulse (120 fs) at the wavelength  $1.5 \mu\text{m}$ , leading predominantly to third-harmonic generation (THG). It has been shown that strong surface plasmon resonance in a nanoslit allows the realization of an effective nanolocalized source of third-harmonic radiation. We show also that a nanoslit in a metal film has a significant advantage in nonlinear processes over its Babinet complementary nanostructure (nanorod): the effective abstraction of heat in a film with a slit makes it possible to use much higher laser radiation intensities.

(Some figures may appear in colour only in the online journal)

## 1. Introduction

Among the important issues and directions of investigation in nano-optics and nanoplasmonics are nonlinear photoproceses [1–3] that can be controlled and manipulated at the nanometer scale. A variety of nonlinear photoproceses in nanoplasmonics has already been explored: (1) second-harmonic generation from metal nanostructures [4–9]; (2) enhanced four-wave mixing on metal surfaces [10]; (3) ultrafast all-optical modulation based on third-order nonlinearity [11–14]; (4) plasmon-enhanced generation of high harmonics [15, 16].

The simplest nonlinear effect which is allowed in all media and independent of nanostructure symmetry is

third-harmonic generation (THG). Nonlinear susceptibility originates from a metal's free electrons: the physics of THG in metals results from the fact that during the oscillations the electron cloud juts out from the ionic core. The resulting restoring force is no longer linear but contains nonlinear terms, starting with the third-order term in the displacement of the center of mass of the electron cloud from its equilibrium position. This collective electron motion near the sharp-edged nanostructure surface is responsible for THG [17].

Apart from its purely fundamental interest, third-harmonic generation in nano-objects is also of considerable practical interest as a nanosized source of short-wavelength radiation [18] or in microscopy for single biomolecule tracking [19].

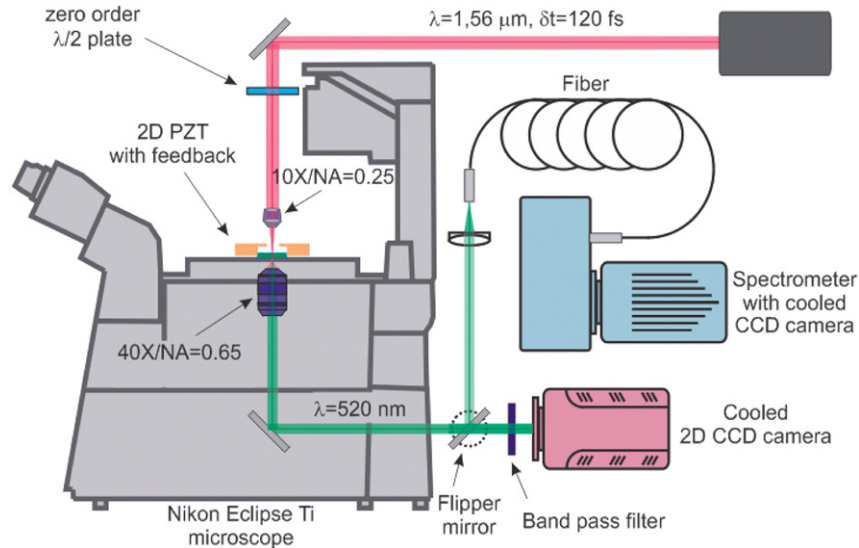


**Figure 1.** Scheme of an experimental setup for investigating third-harmonic generation in single nano-openings.

The most important parameters of third-harmonic generation are the following: (1) the efficiency (the ratio of harmonic power to the exciting radiation power); (2) the efficiency per mass unit, to realize a high yield of THG generated from nanometer scale objects. In experiments [17] THG has been observed in the interaction of relatively weak (intensity  $10^{10}$ – $10^{11}$  W cm $^{-2}$ ) laser radiation with gold nanoparticles. The frequency of the fundamental field used in these experiments was chosen to be one third of the Mie resonance frequency in order to allow a resonant enhancement of the third harmonic. Nevertheless, in this case the THG signal from a single nanoparticle is rather weak, in absolute terms. However, as predicted in [20], for a high intensity ( $10^{16}$  W cm $^{-2}$ ) the internal electric field strength of the third-harmonic amplitude could be of the same order as the field of the fundamental.

It has been recently shown that nanoantennas are excellent nonlinear emitters of light [21]. An essential disadvantage of antennas (and similar nanostructures) as radiation sources is the presence of a considerable accompanying background of exciting radiation at the fundamental frequency and the destruction of the nanostructure at a high incident radiation power, thus presenting a limitation on the efficiency of third-harmonic generation. A nano-object that can generate the third harmonic and, at the same time, is free of the above-mentioned disadvantages is a nano-opening (nano-hole, nanoslits, ...) in a metal film.

In this work we report on a particularly strong optical nonlinearity at the nanometer scale in aluminum and effective third-harmonic generation from single nano-openings in the form of a slit, made in aluminum and also in gold films. We have investigated the effect of the nano-opening geometry on the efficiency of third-harmonic generation. Also we have demonstrated the possibility of constructing a nanolocalized radiation source on their basis, free of a laser radiation background.

## 2. Experimental setup and THG measurements from single nanoslit

The experimental setup is shown schematically in figure 1. The third harmonic was excited by a fiber-coupled femtosecond laser [22] (wavelength 1560 nm, pulse duration 120 fs, pulse rate 70 MHz, mean radiation power incident on the sample 15 mW). The third-harmonic generation was measured using an inverted microscope (Nikon Eclipse Ti). The laser radiation, focused by the objective ( $10\times$ , NA = 0.25) into a spot 4.3  $\mu\text{m}$  in diameter on the sample, was directed transversely to the surface of a film with nano-openings. The peak radiation intensity on the sample was on the order of  $1.1 \times 10^{10}$  W cm $^{-2}$ . To control the polarization of the incident radiation before the focusing objective a zero-order  $\lambda/2$  phase plate was used. The third-harmonic signal was collected using the objective ( $40\times$ , NA = 0.65).

We investigated the third-harmonic generation from the following nano-objects: thin films, single nanoslits in aluminum and gold. The gold was chosen as a well-known nonlinear material in nanoplasmatics, to address the measured efficiency of the THG process in aluminum. For quantitative measurements of the efficiency of third-harmonic generation it is very important to control the focused diameter of the exciting radiation since the efficiency of this process is dependent on the third power of the intensity of the radiation at the fundamental frequency. Therefore, in our measurements the spatial position of the exciting radiation focus was fixed. To study THG a sample with a single nanoslit was moved to the position of a focused laser spot using a 2D piezocontrol system with feedback sensors (CAP201XY, Piezo Jiena). The system provided long-term control over the spatial position of the sample with an accuracy better than 10 nm. The focused laser spot size was measured by spatial scanning of a 100 nm nano-hole across the laser spot and registration of the emission at the fundamental frequency passing through the hole.

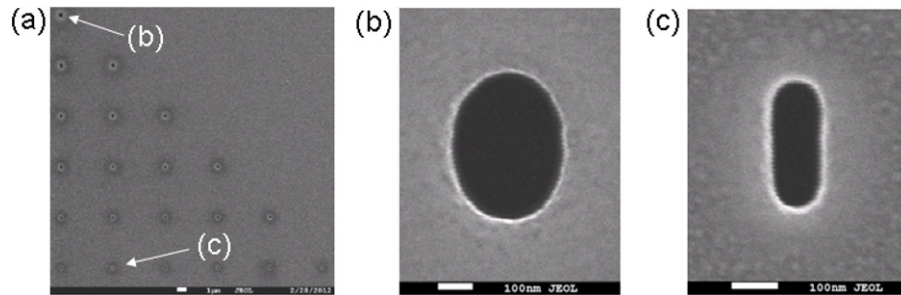


**Figure 2.** (a) Electron microscope image of an array of nanoslits made in Al film; (b), (c) electron microscope images of individual nanoslits indicated by arrows on figure 2(a).

A set of interference and color filters was used for suppression of the exciting laser radiation at 1560 nm wavelength. The radiation at the exciting frequency was suppressed also due to the chromatic aberration of the objective lens, which becomes considerable because of a large difference in radiation wavelengths at the fundamental frequency and at the third-harmonic frequency. Finally the signal registered at the fundamental frequency was suppressed by more than 13 orders of magnitude. The spatial distribution of the third-harmonic radiation was registered by a 2D cooled CCD camera (Princeton Instruments, Photon-MAX) with an avalanche gain of electrons. The signal registered by the 2D CCD camera was carefully calibrated to perform quantitative measurements of the THG radiation power. The emission spectrum from samples was measured using a spectrometer with a cooled CCD camera (Princeton Instruments, NTE/CCD-1340/100). At the spectrometer input the signal was subjected to spatial filtration, which allowed the reduction of the background contribution to the radiation spectrum under registration. The whole setup was placed on a vibration-isolated table to eliminate the effect of mechanical perturbation.

Al and Au films were deposited on the surface of ultrathin (40 nm thick)  $\text{SiO}_2$  membranes with low roughness ( $<1.5 \text{ \AA}$ ) [23], which in turn leads to the metal films adjacent to the membrane having the same small roughness. The high quality of the metal surface close to the membrane enabled the minimization of the contribution of photoluminescence from the roughness of the metal surface in the signal being registered. For this purpose, in all the measurements, the smooth side of the films was facing the radiation at the fundamental frequency. Third-harmonic generation was investigated in nano-openings in 50 nm thick Au and Al films. There are two main reasons for the chosen film thickness: (1) it enables the reduction of the radiation attenuation in the channel formed by the small-diameter nano-opening, which is essential to realize a high efficiency of THG in a nano-opening, (2) Fabry-Perot like resonances (formed by the reflection of radiation from the metal-dielectric boundary) are not realized, which in turn would result in variations in the efficiency of nonlinear processes [24]. Moreover, in metal films 10–100 nm thick the generation of radiation at the third-harmonic frequency can be described analytically [25].

Aluminum films were formed by e-beam evaporation. Gold films were produced by thermal evaporation at  $1240^\circ\text{C}$

under high vacuum. The thickness of the Al and Au films was equal to  $50 \pm 5 \text{ nm}$  and was measured by an atomic force microscope using the razor blade scratch technique. The measured roughness of the Au film surface is as follows: a height roughness (RMS) of about 3 nm and a lateral roughness (correlation length) of about 30 nm. The measured roughness of the Al film surface is as follows: a height roughness of about 1.5 nm and a lateral roughness of about 5 nm. The samples were prepared under the conditions of a Class 100 clean room; the optical measurements were performed under the conditions of a Class 1000 clean room.

In our work we studied nanoslits with aspect ratios in the range 1–5 made in 50 nm thick Al and Au films. Nanoslits were produced using a  $\text{Ga}^+$  beam, 30 keV (FEI Quanta 3D) focused on the surface of an Al (Au) film into a spot with diameter of about 10 nm. The microscopy of the nanoslits was conducted by a JEOL JSM-7001F electron microscope with a spatial resolution of about 5 nm. To reduce the intensity of carbon deposition associated with electron beam microscopy of metallic surfaces the process was carried out at a relatively low electron beam energy of about 5 keV. As an example, figure 2 shows typical samples used in our studies. To avoid the influence of collective plasmonic effects the distance between the nanoslits was about  $5 \mu\text{m}$ . The distance between the nanoslits also exceeded the spot diameter of laser radiation at the fundamental frequency. The order in which the nanoslits were arranged permitted us to identify each individual nanoslit and to work individually with them.

### 3. Third-order optical nonlinearity of Al

Gold is one of the main materials for constructing elements of nanoplasmonics. In [26], however, it has been shown lately that aluminum has certain advantages over gold since it exhibits strong nonlinear properties when it is excited at 780 nm, which, however, is inside of an absorption band of aluminum. The exciting radiation used in this work (1560 nm) is tuned far from the interband electron transition both in gold and aluminum. It is known that at a wavelength of 1560 nm aluminum has stronger metallic properties than gold: the refractive index of Al has a higher real part and a considerably smaller imaginary part compared to Au. Hence, a corresponding difference in the nonlinear optical properties can be expected.

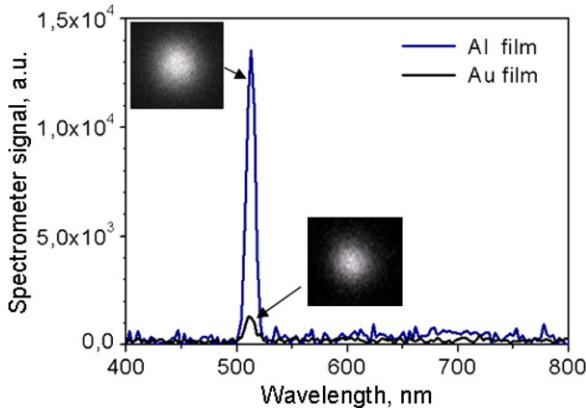


**Figure 3.** THG emission spectra from Al (blue curve) and Au (black curve) films. Excitation laser wavelength 1560 nm. The insets show two-dimensional optical images formed by THG radiation, with exciting laser radiation focused into a spot of  $4.3 \mu\text{m}$  in diameter.

Figure 3 shows measured spectra of third-harmonic generation in Al and Au films without nano-openings. The laser radiation at the fundamental frequency was focused onto the film surface. The radiation at the third-harmonic frequency that has passed through the film was registered by a 2D CCD. The image is in the form of a spot, about  $2 \mu\text{m}$  in diameter, which is about  $\sqrt{3}$  times less than the diameter of the focused laser beam, since the efficiency of the THG signal is third-power dependent on the intensity of radiation at the fundamental frequency. Due to center symmetry, there is no signal corresponding to a second-order response detected. In the spectra of figure 3 the third-order response is dominant. It can be seen that the signal at the third-harmonic frequency in the Al film is twelve times higher than in the Au film.

Our measurements and calculations show that the transmission of the Au film at 520 nm is higher than that of the Al film by 700 times. This indicates that the efficiency of third-harmonic generation in Al is considerably higher, by several orders, than that in Au. The thickness of the films chosen is considerably less than  $\lambda/4\pi$ , and therefore the contribution of the dielectric/metal boundary into nonlinear susceptibility exceeds the pertinent contribution of the material volume [27]. Under such an assumption we have determined the nonlinearity factor  $\chi^{(3)}$  by measuring the radiation intensity at the basic frequency and at the frequency of third-harmonic generation. The measured absolute values of third-harmonic radiation intensity are  $I_{\text{Au}}(3\omega) = 3.3 \times 10^2 \text{ W m}^{-2}$  for Au and  $I_{\text{Al}}(3\omega) = 4.1 \times 10^3 \text{ W m}^{-2}$  for Al. Using the numerical coefficients  $\chi^{(1)}(3\omega) = -4.17 + 3.2i$  for Au [28] and  $\chi^{(1)}(3\omega) = -39.2 + 10.9i$  for Al [29] we have the following coefficient values:  $\chi_{\text{Au}}^{(3)} = (2.3 \pm 0.7) \times 10^{-20} \text{ m}^2 \text{ V}^{-2}$ ,  $\chi_{\text{Al}}^{(3)} = (2.6 \pm 0.8) \times 10^{-17} \text{ m}^2 \text{ V}^{-2}$ . Details of these calculations can be found elsewhere [30].

To our knowledge, these are first measurements of third-order nonlinearity coefficients for Au and Al excited at 1560 nm. The theoretical calculations [31] for the radiation at the fundamental frequency of  $1.06 \mu\text{m}$  predict that the value of third-order nonlinear susceptibility for Al is 40

times higher than for Au. The ratio measured in our work comes to about  $10^3$ . We explain the difference by the spectral dependence of the  $\chi^{(3)}$  coefficient: the metallic properties of aluminum are much stronger at  $1.56 \mu\text{m}$  than at  $1.06 \mu\text{m}$ . The measured difference of the  $\chi^{(3)}$  coefficient for Al and Au can be explained by the difference in the physical and optical properties of the two metals [26]: (1) a difference in the polycrystalline structure of the metals [32] (the characteristic size of the crystal  $\sim 20 \text{ nm}$  for gold and  $\sim 80 \text{ nm}$  for aluminum), (2) a difference in the electron energy level structure and the associated interband transitions [33].

#### 4. Effective nanolocalized source of third-harmonic radiation based of a single nanoslit

A single nanoslit can display several plasmonic resonances, since the frequency of resonance depends on the nanoslit geometry [34]. As shown [35], with the proper geometry of the structure it is possible to realize resonance conditions at scattering both at the fundamental frequency and at the second-harmonic radiation frequency, which causes a considerable increase of the second-harmonic generation efficiency. According to [36], such a technique of double resonance realization can also be applied to increase generation of radiation at the third harmonic from a single nanoslit.

Our calculations show that for radiation at the fundamental frequency a plasmon resonance on single nanoslit in an aluminum film is realized for nanoslit length about 600 nm. A nanoslit with such a length forms a light source with a spatial size of subwavelength levels and thus has no practical value for the realization of a nanolocalized source of light. Therefore, we have chosen the strategy to support plasmon resonance at the THG frequency. The proper geometry of the nanoslit to realize plasmon resonance at the THG geometry was determined through computer simulation, using the Finite Integration Technique (FIT) of transmission of a plane monochromatic wave with its wavelength corresponding to third-harmonic generation (520 nm) and the wavevector orthogonal with respect to the slit plane. The incident light polarization was taken to be transverse to the long axis of the slit. From the computer simulation we have found that a slit 170 nm long and 50 nm in width in 50 nm thick Al foil has a resonance in transmission at the THG wavelength. Figure 4(a) shows the electric field distribution calculated by FIT when this slit is exposed to monochromatic radiation at a wavelength of 520 nm with the polarization directed across and along the long axis of the slit. It is evident that the field becomes more intense when the excitation radiation is polarized across the long axis of the slit.

We prepared nanoslits in 50 nm thick aluminum film with a size of  $50 \text{ nm} \times 170 \text{ nm}$ . The result of measuring third-harmonic generation from one of these slits is given in figure 4(b). The analysis of spatial optical images shows that the signal consists of two parts: (1) a wide pedestal formed by third-harmonic generation in the film, with a size determined by the spot size of the exciting laser radiation, and (2) a narrow

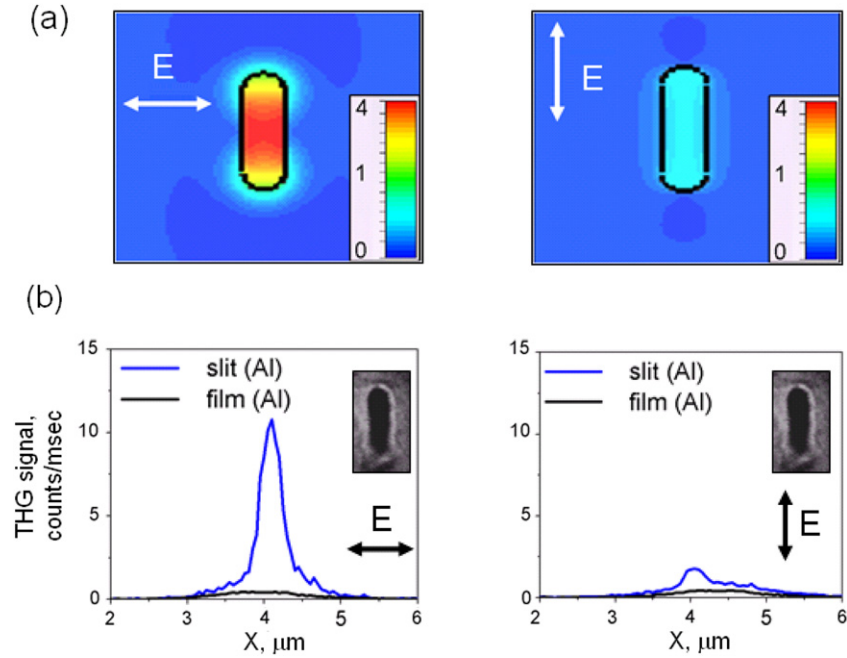


**Figure 4.** Third-harmonic generation from a slit of size  $50 \text{ nm} \times 170 \text{ nm}$  made in an aluminum film  $50 \text{ nm}$  thick with two different polarizations of radiation: left column—polarization is directed across the long axis of the slit; right column—polarization along the long axis. (a) Electric field amplitude enhancement inside a nanoslit irradiated by a plane monochromatic wave at the third-harmonic generation frequency (calculations); (b) measured profiles of a two-dimensional optical images of a nanoslit formed by THG radiation from the nanoslit (blue curve) and by THG radiation from a  $50 \text{ nm}$  thick Al film without a nanoslit (black curve). The inset shows a nanoslit image in an electron microscope.

diffraction-limited peak formed by THG radiation originating from the nanoslit. It is clear to see that the THG signal excited by the radiation with the polarization across the main axis of the slit significantly exceeds the signal with the polarization along the axis. When the nanoslit is subjected to exciting radiation with the polarization across the slit the efficiency of THG radiation corresponding to a unit square (ratio of field intensity of THG radiation to the intensity of the field on the fundamental frequency) is several orders of magnitude higher compared to the THG efficiency from a smooth surface (black curve on figure 4(b)). The role of excitation of plasmon resonance on the high efficiency of THG process was verified in a different experiment. We measured the efficiency of THG from Al nanoslits with different aspect ratios and found that the maximum efficiency of THG is realized on a nanoslit with its geometry optimized in computer simulations to support plasmon resonance (presented on figure 4). At first sight, this is counter-intuitive, as the removal of nonlinear material (the metal) enhances the THG response [37]. This finding is related to the excitation of plasmon resonances and the corresponding increase of the local electric field.

When comparing the THG signals from the nanoslit and the Al film without the nanoslit, it is necessary to take into account that the profiles in figure 4(b) (which corresponds to the THG from the nanoslit) are diffraction limited. Therefore, the ratio between the THG efficiency from the nanoslit and from the Al film is, in fact, considerably higher than the value that follows from a comparison of the two signal amplitudes in figure 4(b). For a nanoslit in Al the measured THG efficiency (corresponded to a unit square) is about

$10^{-9}$ , which is about 2 orders of magnitude higher than the measured THG efficiency in the Al film. For the gold sample the corresponding efficiency for a nanoslit of the same geometry, but made in a  $50 \text{ nm}$  thick gold film, was  $\sim 7 \times 10^{-10}$  and about 3 orders of magnitude higher than the measured THG efficiency in the Au film. That is we measure a comparable signal of THG in slits made in Al and Au films, although the nonlinear properties of aluminum are much stronger than those of gold. Our calculations of electric field enhancement inside aluminum and gold nanoslits show that the plasmon resonance in Au is much stronger than in Al at the wavelength of THG radiation, leading to a greater increase of the local electric field amplitude and hence a higher THG signal. The amplitude of the local field enhanced by excitation of plasmonic oscillations is also affected by the volume and surface roughness induced losses [38]. We expect that slit boundary quality should also affect the THG efficiency.

A greater gain in the efficiency of the THG from the nanoslit can be realized by increasing the exciting laser light, since the THG signal depends on the intensity to the third power. However, this approach is limited by destruction of the nanostructure under intense radiation. In [16, 17, 19], the change in the geometry of gold nanorods under intense femtosecond laser radiation was studied and it was found that the nanostructure geometry did not change up to intensities  $\sim 10^{10} \text{ W cm}^{-2}$ . At higher intensities the metal begins to melt, which causes the nanorod shape and, hence, its resonant properties to change as well. According to the Babinet principle for PEC nanostructures, light scattering

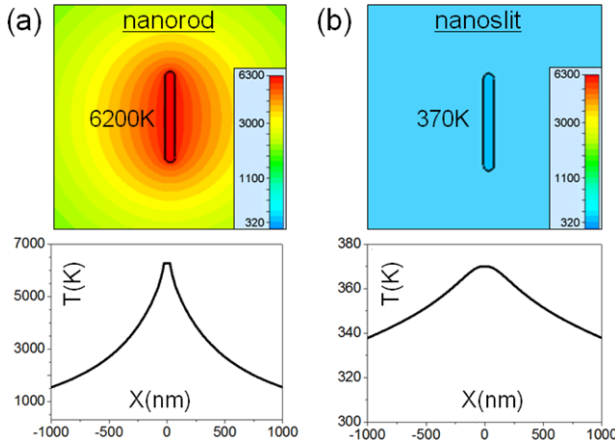


**Figure 5.** Calculated 2D spatial temperature distribution and its one-dimensional cross-section in the following nanostructures exposed to laser radiation with an intensity  $8 \times 10^{13} \text{ W cm}^{-2}$ : (a) aluminum nanorod of size  $50 \text{ nm} \times 50 \text{ nm} \times 570 \text{ nm}$ ; (b) nanoslit of size  $50 \text{ nm} \times 570 \text{ nm}$  in a  $50 \text{ nm}$  thick aluminum film.

on a nanorod is identical to nanoslit transmission (with the appropriate substitution of radiation polarization). However, the thermal behavior of nanostructures and nano-openings at high laser intensities differ significantly. Below we show that the effective heat withdrawal in a film makes it possible to use much higher laser powers with nanoslits than with nanorods when the sample is not melted yet.

Figure 5(a) shows the spatial temperature distribution in an aluminum nanorod of size  $50 \text{ nm} \times 570 \text{ nm}$ . The data were obtained through numerical solution of the heat conduction equations using FIT calculations. Figure 5(b) shows a similar distribution for a nanoslit of the same size in a  $50 \text{ nm}$  thick aluminum film. Both the structures are exposed to a plane monochromatic wave, with a wavelength of  $1560 \text{ nm}$  and the wavevector orthogonal to the nanostructure plane. The laser intensity is  $8 \times 10^{13} \text{ W cm}^{-2}$ . The geometry of the nanostructures of figure 5 was chosen to support excitation of plasmonic oscillations by  $1560 \text{ nm}$  radiation. The radiation polarization for the nanorod is directed along its long axis and for the nanoslit across its length so that resonant excitation of plasmon oscillations can be realized. It can be seen from the figure that the nanorod is heated to much higher temperatures than the slit, while the radiation intensities are the same. These calculations show that it is impossible to use nanorods at high radiation intensities (due to their destruction), which, in turn, means that the efficiencies of THG on such an object will differ drastically.

Further calculations [30] based on the measurement performed in this work show that in a nanoslit in aluminum, with the proper chosen geometry, exciting radiation intensity of the order of  $10^{13} \text{ W cm}^{-2}$  will lead to realization of the THG efficiency of the process being on the order of unity. We stress that this intensity is three orders of magnitude higher than the maximum intensity that would lead to the melting of metallic nanostructures [16, 17, 19]. Thus the effective removal of heat in a film makes it possible to use a much higher laser light intensity and to realize a much higher THG efficiency with nanoslits than with nanorods.

## 5. Conclusions

In conclusion, we have demonstrated THG for single nanoslits made in aluminum and gold films. We have measured and compared the THG efficiency from these two nano-objects and, as a result, we have obtained absolute values of nonlinear third-order susceptibility for aluminum and gold. It has been found that the presence of plasmon resonances in nanoslits allows a considerable increase in THG efficiency. This in turn allows the realization of a background free nanolocalized source of third-harmonic radiation. Finally, we would like to stress that nonlinear optical materials in the form of nanosized objects are of great practical importance for future applications in optical signal processing, optical imaging with nanometer resolution and nonlinear optical devices [39–43].

## Acknowledgments

We are grateful to P Starikov for sputtering the thin Al films used in these experiments. This work was partially supported by the Russian Foundation for Basic Research, grant nos 11-02-00804-a, 12-02-00784-a, and by the Program ‘Extreme Light Fields’ of the Presidium of the Russian Academy of Sciences. This work was performed using equipment of the CKP ISAN, CKP MIPT with the financial support of the Ministry of Education and Science of the Russian Federation.

## References

- [1] Novotny L and van Hulst N 2011 *Nature Photon.* **5** 83
- [2] Schumacher T, Kratzer K, Molnar D, Hentschel M, Giessen H and Lippitz M 2011 *Nature Commun.* **2** 333
- [3] Schuller J A, Barnard E S, Cai W, Jun Y C, White J S and Brongersma M L 2010 *Nature Mater.* **9** 193
- [4] Palomba S, Danckwerts M and Novotny L 2009 *J. Opt. A: Pure Appl. Opt.* **11** 114030
- [5] Bouhelier A, Beversluis M, Hartschuh A and Novotny L 2003 *Phys. Rev. Lett.* **90** 013903
- [6] Labardi M, Allegrini M, Zavelani-Rossi M, Polli D, Cerullo G, Silvestri S D and Svelto O 2004 *Opt. Lett.* **29** 62
- [7] Stockman M I, Bergman D J, Anceau C, Brasselet S and Zyss J 2004 *Phys. Rev. Lett.* **92** 057402
- [8] Zheludev N I and Emelyanov V I 2004 *J. Opt. A: Pure Appl. Opt.* **6** 26
- [9] Canfield B K, Husu H, Laukkonen J, Bai B F, Kuitinen M, Turunen J and Kauranen M 2007 *Nano Lett.* **7** 1251
- [10] Renger J, Quidant R, van Hulst N and Novotny L 2010 *Phys. Rev. Lett.* **104** 046803
- [11] Utikal T, Stockman M I, Heberle A P, Lippitz M and Giessen H 2010 *Phys. Rev. Lett.* **104** 113903
- [12] Pacifici D, Lezec H J and Atwater H A 2007 *Nature Photon.* **1** 402–6
- [13] MacDonald K F, Samson Z L, Stockman M I and Zheludev N I 2009 *Nature Photon.* **3** 55
- [14] Liu Z Y, Ding P J, Shi Y C, Lu X, Liu Q C, Sun S H, Liu X L, Ding B W and Hu B T 2012 *Laser Phys. Lett.* **9** 649
- [15] Kim S, Jin J H, Kim Y J, Park I Y, Kim Y and Kim S W 2008 *Nature* **453** 757
- [16] Park I Y, Kim S, Choi J, Lee D H, Kim Y J, Kling M F, Stockman M I and Kim S W 2011 *Nature Photon.* **5** 677
- [17] Fomichev S V and Becker W 2010 *Phys. Rev. A* **81** 063201
- [18] Ganeev R A 2012 *Laser Phys. Lett.* **9** 175

- [19] Lippitz M, Dijk M and Orrit M 2005 *Nano Lett.* **5** 799
- [20] Fomichev S V, Popruzhenko S V, Zaretsky D F and Becker W 2003 *J. Phys. B: At. Mol. Opt. Phys.* **36** 3817
- [21] Hanke T, Cesar J, Knittel V, Trügler A, Hohenester U, Leitenstorfer A and Bratschitsch R 2012 *Nano Lett.* **12** 992
- [22] Femtosecond Laser 2011 *EFOA-SH* Avesta
- [23] Melentiev P N, Zablotskiy A V, Lapshin D A, Sheshin E P, Baturin A S and Balykin V I 2009 *Nanotechnology* **20** 235301
- [24] Renger J, Quidant R and Novotny L 2011 *Opt. Express* **19** 1777
- [25] Fomichev S V, Zaretsky D F and Becker W 2009 *Phys. Rev. B* **79** 085431
- [26] Castro-Lopez M, Brinks D, Sapienza R and Van Hulst N F 2011 *Nano Lett.* **11** 4674
- [27] Boyd R W 2003 *Nonlinear Optics* (London: Academic) p 127
- [28] Johnson P B and Christy R W 1972 *Phys. Rev. B* **6** 4370
- [29] Rakic A D 1995 *Appl. Opt.* **34** 4755
- [30] Konstantinova T V, Melentiev P N, Afanasiev A E, Kuzin A A, Baturin A S, Tausenev A V, Konyaschenko A V and Balykin V I 2013 *JETP* at press
- [31] Burns W K and Bloembergen N 1971 *Phys. Rev. B* **4** 3437
- [32] Boyd G T, Yu Z H and Shen Y R 1986 *Phys. Rev. B* **33** 7923
- [33] Palik E D 1985 *Handbook of Optical Constants of Solids* vol I (Orlando, FL: Academic)
- [34] Popov E and Bonod N 2011 *Structured Surfaces as Optical Metamaterials* ed A A Maradudin (Cambridge: Cambridge University Press) pp 1–27
- [35] Nakanishi T, Tamayama Y and Kitano M 2012 *Appl. Phys. Lett.* **100** 044103
- [36] Reintjes J F 1984 *Nonlinear Optical Parametric Processes in Liquids and Gases* (Orlando, FL: Academic)
- [37] Schön P, Bonod N, Devaux E, Wenger J, Rigneault H, Ebbesen T W and Brasselet S 2010 *Opt. Lett.* **35** 4063
- [38] Raether H 1986 *Surface Plasmons on Smooth and Rough Surfaces and on Gratings* (Berlin: Springer) p 51
- [39] Chen W-J, Wang H-Z, Lin R-Y, Lee C-K and Pan C-L 2012 *Laser Phys. Lett.* **9** 212
- [40] Lepeshkin N N, Kim W, Safonov V P, Zhu J G, Armstrong R L, White C W, Zuhir R A and Shalaev V M 1999 *J. Nonlinear Opt. Phys. Mater.* **8** 191
- [41] Melentiev P N, Afanasiev A E, Kuzin A A, Zablotskiy A V, Baturin A S and Balykin V I 2011 *Opt. Express* **19** 22743
- [42] Melentiev P N, Konstantinova T V, Afanasiev A E, Kuzin A A, Baturin A S and Balykin V I 2012 *Opt. Express* **20** 19474
- [43] Zheltikov A M 2004 *Laser Phys. Lett.* **1** 220–33